BBA - Biomembranes 1862 (2020) 183015

Contents lists available at ScienceDirect

BBA - Biomembranes

journal homepage: www.elsevier.com/locate/bbamem

Revisiting a controversy: The effect of EGF on EGFR dimer stability☆

Deo R. Singh[a,b], Christopher King[a,c], Matt Salotto[b], Kalina Hristova[a,b,c,*]

[a] Institute of NanoBioTechnology, Johns Hopkins University, 3400 Charles Street, Baltimore, MD 21218, United States of America
[b] Department of Materials Science and Engineering, Johns Hopkins University, 3400 Charles Street, Baltimore, MD 21218, United States of America
[c] Program in Molecular Biophysics, Johns Hopkins University, 3400 Charles Street, Baltimore, MD 21218, United States of America

ARTICLE INFO

Keywords:
Receptor tyrosine kinase
EGFR
EGF
Dimer stability
Thermodynamics

ABSTRACT

EGFR is a receptor tyrosine kinase that plays a critical role in cell proliferation, differentiation, survival and migration. Its activating ligand, EGF, has long been believed to stabilize the EGFR dimer. Two research studies aimed at quantitative measurements of EGFR dimerization, however, have led to contradicting conclusions and have questioned this view. Given the controversy, here we sought to measure the dimerization of EGFR in the absence and in the presence of saturating EGF concentrations, and to tease out the effect of ligand on dimer stability, using a FRET-based quantitative method. Our measurements show that the dissociation constant is decreased ~150 times due to ligand binding, indicative of significant dimer stabilization. In addition, our measurements demonstrate that EGF binding induces a conformational change in the EGFR dimer.

1. Introduction

Receptor Tyrosine Kinases (RTKs) are single-pass membrane proteins with ligand-binding extracellular domains and intracellular kinase domains [1,2]. RTKs play important roles in human development and in cancer [3–6], and are known to transduce biochemical signals via lateral dimerization [7–9]. Dimerization acts to bring two kinases in close proximity, so they can phosphorylate and activate each other. The activated kinases phosphorylate additional tyrosine residues which recruit adaptor proteins and trigger downstream signals that control cell growth, motility, and differentiation.

On the cell surface, RTKs can exist as either monomers or oligomers (usually dimers) [7,10,11]. Reversible dimerization is known to occur even in the absence of ligand, and has been linked to low kinase phosphorylation levels known as basal phosphorylation [12,13]. RTKs become fully activated when they bind their cognate ligands through specific sites on their extracellular domains. It is believed that one of the major roles of the ligand in this process is to stabilize the RTK dimers [8,9,14,15]. Yet, quantitative measurements of dimer stabilities for one of the best studied RTKs, EGFR, have produced contradicting results and have questioned the role of ligand in dimer stabilization [16,17].

EGFR plays a critical role in cell proliferation, differentiation, survival, and migration [18,19]. It has been implicated in many cancers, and has been recognized as an attractive candidate for anticancer therapies [20–22]. EGFR can respond to several ligands, with EGF known to be the most potent. EGF is a monomeric, 53 amino acid residue polypeptide with a characteristic fold that is stabilized by three intramolecular disulfide bonds. It binds the EGFR receptor in 1:1 stoichiometry. EGF has been widely used in structural and biophysical studies, and as a general mitogen in cell culture experiments [23–25].

To gain insights into the molecular interactions between EGF and EGFR molecules, Macdonald and Pike measured EGF binding to cell monolayers that were stably transfected with a plasmid that encoded for EGFR under the control of a tet-inducible promoter [16]. This allowed the researchers to vary both the EGF concentration and the EGFR expression. The binding data were fitted with a model that accounts for both ligand binding and receptor dimerization, yielding all binding and dimerization constants. In the model, unliganded EGFR monomers can dimerize, and ligand can bind to EGFR monomers, to unliganded EGFR dimers, and to singly liganded EGFR dimers. The dissociation constant of unliganded dimerization was determined as ~114 receptors/μm^2 (rec/μm^2). The dissociation constant describing the lateral dimerization of one liganded and one unliganded EGF receptors was found to be similar, which is a surprising finding indicating that the effect of the bound ligand is negligible in this process. Finally, the dissociation constant describing the lateral dimerization of two liganded EGF receptors was higher, ~1340 rec/μm^2, suggesting that the interactions between the EGF receptors were reduced upon ligand binding. The latter results were interpreted as a manifestation of negative

☆ This article is part of a Special Issue entitled: Molecular biophysics of membranes and membrane proteins.

* Corresponding author at: Institute of NanoBioTechnology, Johns Hopkins University, 3400 Charles Street, Baltimore, MD 21218, United States of America.
E-mail address: kh@jhu.edu (K. Hristova).

https://doi.org/10.1016/j.bbamem.2019.07.003
Received 15 March 2019; Received in revised form 23 June 2019; Accepted 2 July 2019
Available online 08 July 2019
0005-2736/

cooperativity in the binding of the second EGF to the EGFR dimer.

An assay, termed "Co-II" and based on single molecule particle tracking, was recently developed by Kim and colleagues and used to visualize the interactions between an immobilized receptor and freely diffusing receptors in the plasma membranes of live cells [17]. The premise behind the dimerization measurements in this assay is that if a receptor is immobilized, its interaction partner will also be immobilized during the lifetime of the complex. With this assay, the dissociation constants in the absence of EGF and in the presence of 100 nM EGF were measured as 1606 ± 332 rec/μm^2 and 122 ± 14 rec/μm^2, respectively. Thus, in the Co-II assay, the presence of 100 nM EGF decreased the dissociation constant, indicating that the bound ligand enhances the interactions between the EGFR molecules and stabilizes the EGFR dimer.

Reports of effective ligand-binding (EGF-EGFR) dissociation constants are typically in the 1–2 nM range [26,27]. 100 nM EGF is therefore expected to saturate all EGFR molecules in the co-II assay. Thus, the dissociation constant measured in the presence of 100 nM EGF in the co-II assay should correspond to the dimerization of ligand-bound EGFR receptors, a regime that was also accessed in the work of McDonald and Pike. Since the two research studies have led to contradicting conclusions, we sought to measure the dimerization of EGFR in the absence and in the presence of saturating EGF concentrations using an alternative technique: a FRET-based quantitative method that is well established [28]. The method has been used previously to study the dimerization of other RTKs, and has been verified with biochemical assays [29–33].

2. Results

EGFR dimerization measurements were performed in the plasma membranes of HEK 293 T cells using the Fully-Quantified Spectral Imaging (FSI) methodology, which yields receptor surface densities and FRET efficiencies in micron-sized regions of the plasma membrane [28,34,35]. We used a truncated version of the EGFR receptor (EGFR ECTM), in which the kinase domain was substituted with fluorescent proteins [36]. The EGFR ECTM construct contained the entire EGFR extracellular (EC) domain, the EGFR transmembrane (TM) domain, a flexible $(GGS)_5$ linker, and a fluorescent protein at the C-terminus. The lack of the kinase domain in this receptor eliminated effects due to phosphorylation-induced endocytosis and recycling/downregulation, allowing straight-forward data interpretation.

The FRET pair of mTurq and YFP was used in the experiments (see Fig. 1A for the emission spectra of the two fluorophores). HEK 293 T cells were co-transfected with EGFR ECTM-mTurq and EGFR ECTM-YFP and imaged in a two-photon microscope equipped with the OptiMis spectral detection system. Following published protocols [28,34], experiments were performed under reversible osmotic stress, to allow the calculations of two-dimensional receptor concentrations in the plasma membrane. As discussed in the literature, the cell membrane of live cells is highly "ruffled" [31,37,38], and the reversible osmotic stress eliminates these ruffles [39]. In the absence of ruffles, the two-dimensional receptor concentrations in the membrane are calculated from the effective three-dimensional receptor concentrations, which are determined using purified fluorescent protein standards [28]. The reversible osmotic stress treatment does not alter the FRET efficiencies, and is completely reversible [28,32].

In total, 500 cells coexpressing EGFR ECTM-mTurq and EGFR ECTM-YFP were imaged in 9 independent experiments. Each individual cell was imaged twice: at 800 nm to excite mTurq and at 960 nm to excite YFP. Complete emission spectra were acquired in both cases. The experimental spectra in each pixel (magenta in Fig. 1B and C) were fitted to a linear combination of the donor and acceptor spectra, acquired in single transfection experiments, as well as a background contribution, to calculate the FRET efficiency and the effective donor and acceptor concentrations in the pixel as described [28]. Pixels within small (μ-sized) regions of homogenous, diffraction-limited plasma membrane fluorescence (Fig. 1D) were analyzed to calculate the average FRET efficiency and the two-dimensional membrane concentrations in the region (see reference (28) for details). Data from many individual cells with different EGFR ECTM expressions were combined to obtain a dimerization curve.

Fig. 2A shows the measured total apparent FRET efficiency in individual cells as a function of EGFR ECTM-YFP (acceptor) concentration in the absence of EGF. Fig. 2B shows the measured EGFR ECTM-mTurq (donor) surface densities as a function of the measured EGFR ECTM-YFP (acceptor) surface densities in these cells. These FRET data were analyzed to determine both the oligomer size and the oligomerization free energy (oligomer stability). The procedure has been described in detail and has been verified [40]. Briefly, association models were built assuming monomers, dimers, or higher order oligomers of order n, and the calculated FRET for each model was compared to the experimental FRET, yielding the mean square errors for the different models. This analysis also takes into account the so-called "proximity" or "stochastic" FRET, which arises due to the random approach of donors and acceptors within 10 nm in the plasma membrane and depends on the oligomer-order, association strength, and intrinsic FRET efficiencies [40–43]. The measured FRET is corrected for this proximity contribution, to obtain the interaction-specific FRET contribution. The latter is a function of the two-dimensional dissociation constant K_{diss} and the structural parameter "Intrinsic FRET" ($\tilde{E}$), which depends on the positioning of the fluorescent proteins in the EGFR oligomer.

Fig. 2C shows the best-fit mean square error (MSE) as a function of the oligomer order. We see that the best fit is achieved when the oligomer order, n, is 2, indicating that a dimerization model yields the best fit to the data. The solid line in Fig. 2D, given by Eq. 8, is the theoretical curve for the best-fit dimer model. The dimeric fractions were calculated from the measured FRET efficiencies and were binned. The averages and the standard errors are shown with the symbols in Fig. 2D. The best-fit value of the two-dimensional dissociation constant is $K_{diss} \approx 2800$ rec/μm^2, corresponding to a dimerization Gibbs free energy of $\Delta G^\circ \approx -3.5$ kcal/mol (see Eq. (10)). The Intrinsic FRET value is $\widetilde{E} \approx 0.80$ (see Table 1)

We next sought to perform the same FRET experiment with EGFR ECTM, but in the presence of saturating amounts of EGF. We used 5 μg/mL, or 780 nM EGF, which is much higher than concentrations used in the literature, and was meant to ensure that all EGFR molecules have ligands bound to them. The FRET efficiency is shown in Fig. 3A as a function of the acceptor concentration with the purple symbols. The donor concentration versus the acceptor concentration is shown in Fig. 3B. The data were analyzed to determine the best-fit oligomerization model as described above. Fig. 3C shows that the overall best-fit MSE occurs at $n = 2$, as in the ligand-free experiments, indicative of dimer formation. Fig. 3D shows the EGFR dimerization curve in the presence of EGF (purple), along with the EGFR dimerization curve in the absence of ligand.

The best-fit two-dimensional dissociation constant for EGFR ECTM domains in the presence of saturating EGF, K_{diss}^{EGF}, is ~19 receptors per μm^2, corresponding to a Gibbs free energy of dimerization, $\Delta G^\circ \approx -6.5$ kcal/mol. Thus, the dissociation constant is reduced about 150 times and the corresponding EGFR dimer stability is enhanced by about −3.0 kcal/mol in the presence of EGF. The best-fit intrinsic FRET value for the dimer is $\widetilde{E} = 0.49$, which is significantly lower than the intrinsic FRET obtained for unliganded EGFR dimers ($\widetilde{E} = 0.81$). The distance between the fluorescent proteins, calculated under the assumption of free rotation, is increased by about 12 Å, from about 43 Å to 55 Å (see Table 1). The fluorescent proteins are attached via flexible linkers to the C-termini of the TM domains, and our measurements thus indicate that the C-termini move away from each other upon ligand binding (Fig. 4). This type of movement is consistent with the current understanding of the conformational changes in the EGFR TM dimer portion upon ligand binding [44,45]. Presumably, this

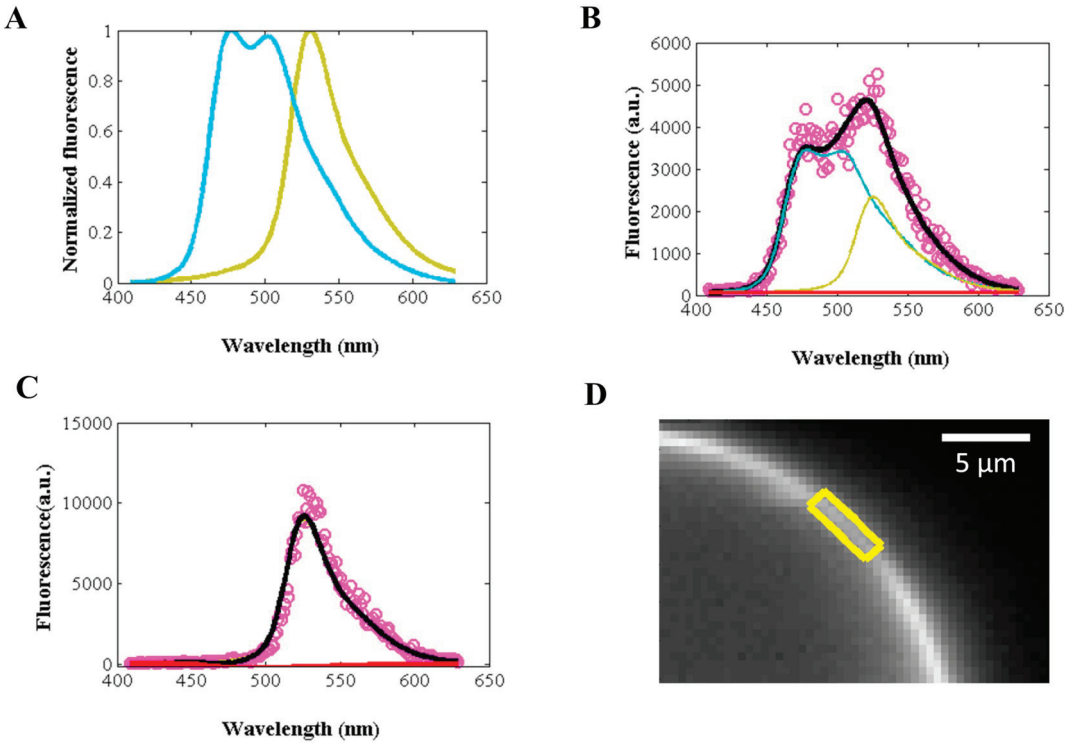

Fig. 1. The FSI method, applied to EGFR ECTM in cells under reversible osmatic stress. (A) Emission spectra of mTurq (cyan) and YFP (yellow). (B) A section of the integrated image of a HEK293T cell under reversible osmatic stress co-expressing EGFR ECTM-mTurq and EGFR ECTM-YFP under excitation at 800 nm. A diffraction-limited region of homogeneous membrane fluorescence, ~3 µm in length (yellow), is analyzed to produce a data point in Fig. 3A and B. (C and D). A single pixel fluorescence (magenta) in the FRET (C) and the acceptor (D) scans is decomposed into a linear sum (black line) of the donor (cyan line), acceptor (yellow line), and background (red line) contributions.

conformational switch is responsible for the full activation (phosphorylation) of the receptor in the presence of saturating EGF.

3. Discussion

To address a controversy in the literature, we sought to determine two equilibrium constants describing EGFR dimerization. In the absence of ligand, we measure a dissociation constant, K_{diss}, which reports on the stability of the unliganded EGFR ECTM dimer, as it describes the equilibrium between unliganded monomers and dimers (Fig. 4, top). In the presence of saturating EGF concentration, we measure a dissociation constant, K_{diss}^{EGF}, which reports on the stability of the fully liganded EGFR dimer, i.e., it describes the equilibrium between liganded monomers and fully liganded dimers (Fig. 4, bottom). These two measurements allow us to quantify the effect of bound EGF on EGFR dimer stability.

The experimental design ensured that we have no EGF ligand unless EGF is added by us. In particular, cells were starved and then the starvation medium was replaced by swelling medium just before imaging. When we add EGF, we add it at very high concentrations to ensure saturation [46].

A direct comparison of the K_{diss} and K_{diss}^{EGF} values in Table 1 to the ones that have been published previously by McDonald and Pike [16] and by Kim and colleagues [17] is not straight-forward, as here we work with EGF receptors that lack the intracellular (IC) domain. By deleting the IC domain, we eliminate any biological effects that may occur as a result of EGFR phosphorylation and complicate data interpretation. The contacts between the IC domains are known to stabilize RTK dimers, but the magnitude of the stabilizing effects can vary between the different RTKs [10,13,45,47–50] and may depend on the presence of bound ligand. Thus, the values of the dissociation constants that we measure for EGFR ECTM could be considered upper estimates of the dissociation constants for full-length EGFR. In the absence of ligand, the value of K_{diss} measured here, ~2800 receptors/µm^2, is slightly higher than the value measured by Kim and colleagues, ~1600 receptors/µm^2, but more than an order of magnitude higher than the one measured by McDonald and Pike, ~110 receptors/µm^2. The values measured in the presence of EGF, K_{diss}^{EGF} vary significantly between the three studies. We measure a value of ~19 receptors/µm^2, as compared to ~120 receptors/µm^2 measured by Kim and colleagues and ~1300 receptors/µm^2 measured by McDonald and Pike. Of the three studies, we measure the strongest dimerization between liganded EGFR molecules. Notably, we use higher EGF concentration, 780 nM, as compared to the other two studies.

In Fig. 3D, we compare the dimerization curves for ECTM EGFR in the presence and absence of ligand. The expression of EGFR has been reported as ~100, ~300, and ~600 receptors/µm^2 in A459, HeLa, and A341 cells, respectively [51]. In Fig. 3D, we see that the EGFR dimeric fraction increases significantly upon EGF addition for these concentrations. It should be kept in mind that the presence of the IC domains will likely stabilize both the unliganded and ligand-bound dimers, and will thus shift both dimerization curves to the left.

To calculate the equilibrium constants and obtain the curves in Fig. 3D, we fit the data with a dimer model (eq. 9). As seen in Figs. 2 and 3, the simple dimer model provides an adequate description of the FRET data and gives the lowest mean square error, as compared to higher oligomer models. This is consistent with a previous report that EGFR forms dimers both in the absence of ligands and in the presence of EGF concentrations exceeding 300 nM [52]. However, it has been suggested that EGFR forms higher order oligomers at low ligand concentrations [52,53]. Therefore, variations in ligand concentrations could lead to variations in the oligomeric state of EGFR. Such variations in the oligomeric state are not accounted for in the thermodynamic model that MacDonald and Pike used to fit their data [16]. It is thus possible that the appearance of reduced EGFR dimer stability upon EGF binding in their experiments is a consequence of the incomplete model

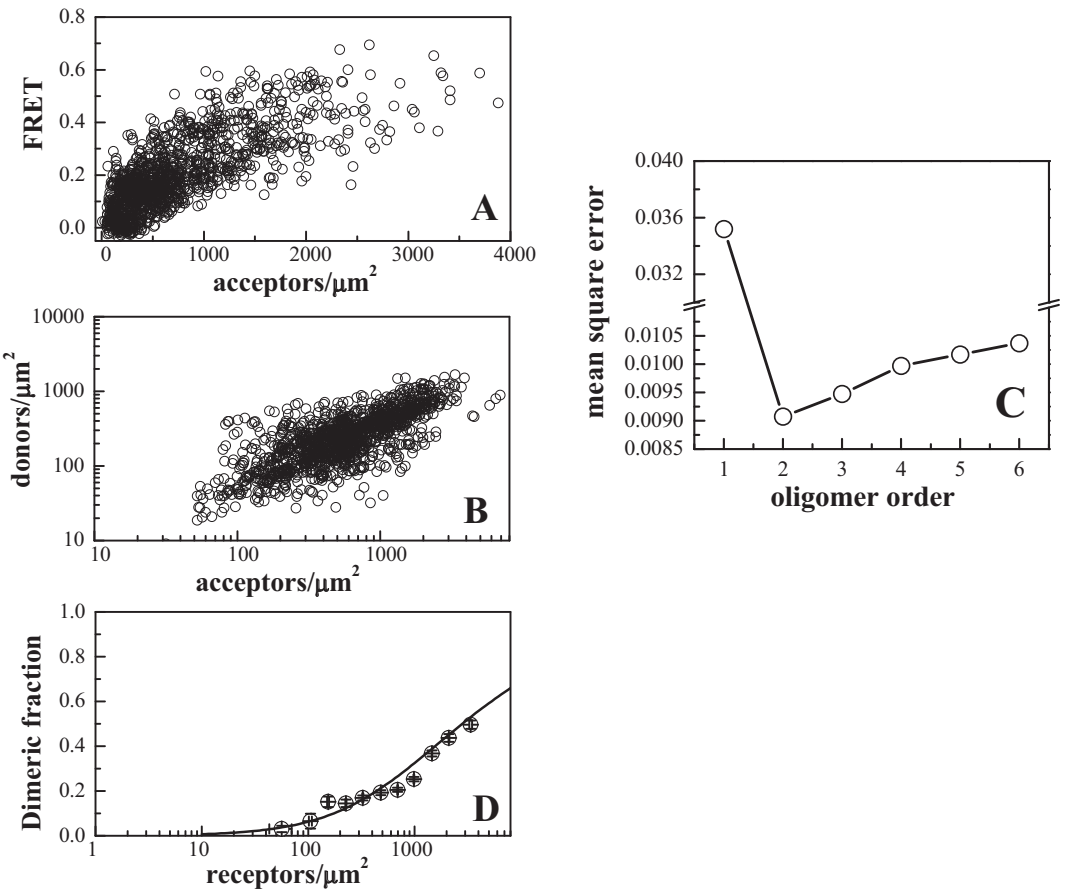

Fig. 2. Dimerization of EGFR ECTM in HEK293T cells, in the absence of ligand. (A) FRET as a function of EGFR ECTM-YFP (acceptor) concentration in the absence of ligand. Each data point represents a single membrane region as in Figure1B. (B) EGFR ECTM-mTurq (donor) concentration versus EGFR ECTM-YFP (acceptor) concentration obtained from each membrane region analyzed, in 500 cells with different receptor expressions. (C) Mean square error (MSE) versus oligomer order in the absence of EGF. The MSE is lowest in the dimer case. (D) Dimeric fraction as a function of EGFR ECTM concentrations. The dimeric fractions measured in individual cells are binned, and the averages and the standard errors are shown with the symbols. The solid line is the theoretical curve for the best-fit dimerization model.

used to fit the ligand binding data.

The FRET efficiencies that we measure in Figs. 2A and 3A depend both on the dimerization constant and on the relative positioning of the fluorescent proteins in the EGFR dimer [54]. The fluorescent proteins in our experiments are attached to the TM domain C-termini via flexible linkers. Thus, the fact that the Intrinsic FRET decreases (the separation between the fluorescent proteins increases) indicates that the separation between the TM domain C-termini increases in response to EGF binding to the EGFR EC domain (see Table 1 and Fig. 4). Previous work has suggested that in the ligand-bound dimer, the EGFR TM domains interact with each other via amino acids close to the N-terminus, and this dimerization mode ensures larger separation of the TM domain C-termini than in the unliganded case [44,45]. Our Intrinsic FRET values, extracted here from the measured FRET efficiencies along with the values of the dissociation constants, are consistent with this view.

In summary, in our hands, the dissociation constant of EGFR is decreased ~150 times due to EGF ligand binding, and the corresponding dimer stability is increased by about −3.0 kcal/mol. This is a substantial increase in dimer stability, as attested by the large increase in dimeric fractions in Fig. 3D. These results are generally consistent with the conclusions of the co-II assay of Kim and colleagues that the stability of the liganded EGFR dimers exceeds the stability of the unliganded dimers, i.e., that ligand binding leads to dimer stabilization [17]. Of note, the effect of EGF on EGFR dimer stability has been explored in other published studies [36,55]. Although the goals of these studies were not measurements of exact dissociation constants, these studies also show that the presence of EGF enhances EGFR dimerization, in line with the results presented here.

4. Materials and methods

4.1. Plasmid construct

EGFR ECTM, tagged with either mTurq or YFP, was subcloned into the pcDNA3.1(+) vector (Invitrogen), as previously described [43]. The EGFR construct consisted of the signal peptide, the entire EGFR EC domain, the EGFR TM domain, a flexible 15 amino acid linker $(GGS)_5$, and either mTurq or YFP at the C terminus.

4.2. Cell culture and transfection

HEK293T cells were purchased from American Type Culture Collection (ATCC) (Manassas, VA, USA). The cells were cultured in Dulbecco's modified Eagle medium (DMEM), supplemented with 10% fetal bovine serum (FBS, Hyclone), 3.5 g/L D-glucose (19.4 mM), and 1.5 g/L (17.9 mM) sodium bicarbonate in 35 mm glass bottom dishes (MatTek Corporation, MA). After twenty four hours, the cells were co-transfected with plasmids encoding EGFR ECTM-mTurq and EGFR ECTM-YFP using Lipofectamine 3000 according to the manufacturer's instructions. After transfection, cells were serum-starved for 12 h. Prior to imaging, the starvation medium was replaced with hypo-osmotic medium to induce osmotic stress and swelling under reversible

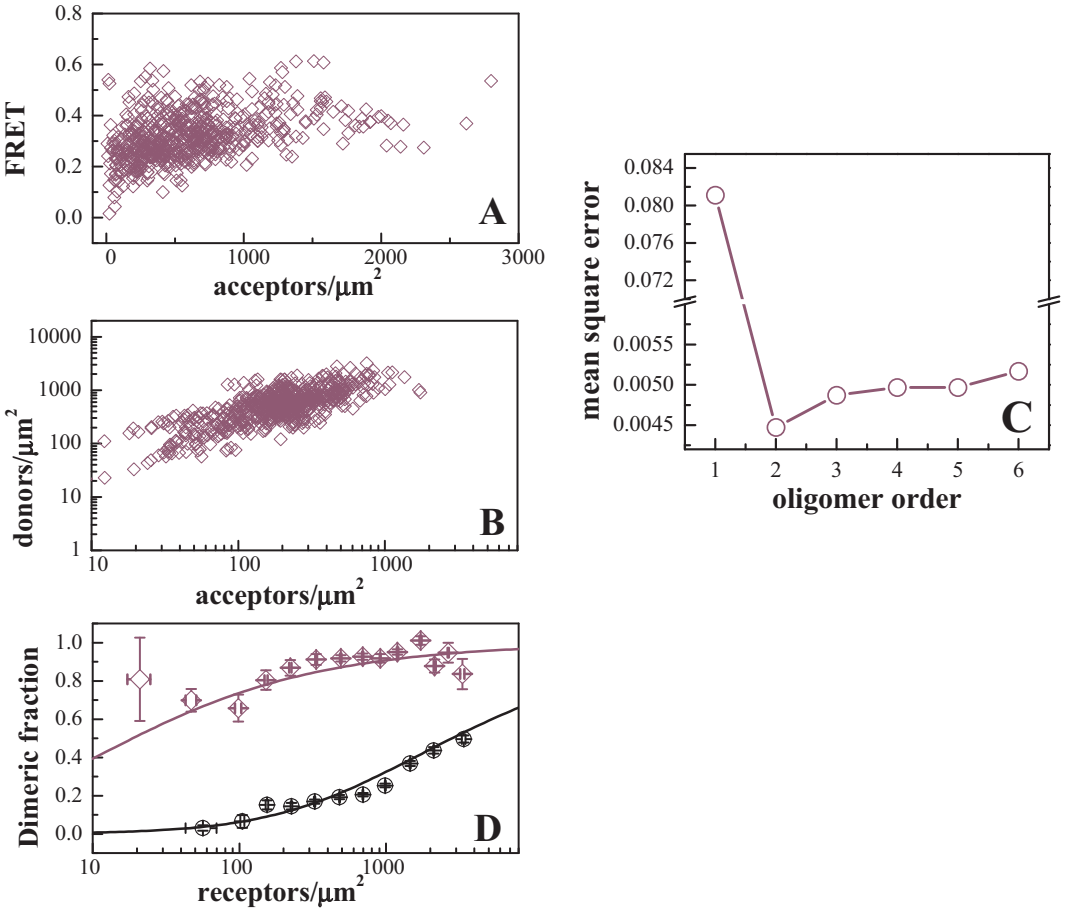

Fig. 3. Dimerization of EGFR ECTM in HEK293T cells, in the presence of 780 nM EGF ligand. (A) FRET as a function of acceptor concentration. (B) Donor concentrations versus acceptor concentrations. (C) MSE versus oligomer order in the presence of EGF. The MSE is lowest in the dimer case. (D) Dimeric fraction as a function of receptor concentrations. The results in the presence of EGF (purple) are compared to the results in the absence of ligand (black).

conditions as described [39]. The cells were allowed to settle down for 10 min and were imaged for two hours. In some experiments, EGF was added at a concentration of 5000 ng/mL (780 nM).

4.3. Two photon microscopy of cells under reversible osmotic stress

Imaging was performed with a spectrally resolved two photon microscope with line-scanning capabilities [56,57]. An ultrashort- pulse laser (MaiTai™, Spectra-Physics, Santa Clara), which generates femtosecond mode locked pulses at wavelengths between 690 nm to 1040 nm, was used as the excitation source for the fluorophores. Cells under reversible osmotic stress were images at 800 nm and 960 nm. The swelling step was necessary because the plasma membrane is highly "wrinkled", as cells possess 2 to 3 times the membrane area needed to sustain their shape [37,38]. When the membrane is "unwrinkled", the effective 3D receptor concentrations, calibrated using purified fluorescent protein solutions of known concentrations, are easily converted into 2D receptor concentrations in the plasma membrane (see ref. (28)).

4.4. FSI method

The methodology has been described in detail in previous work [28]. Briefly, two scans were performed: (1) a FRET scan at wavelength λ_1 (800 nm), which excites primarily the donor and (2) an acceptor scan at wavelength λ_2 (960 nm), which excites primarily the acceptor. Using these two scans and a calibration with purified fluorescence protein standards, we determine the FRET efficiencies, the donor concentrations, and the acceptor concentrations using the following equations:

$$E_{app} = 1 - \frac{F_{\lambda 1}^{DA}}{F_{\lambda 1}^{D}} \quad (1)$$

$$[D] = \frac{F_{\lambda 1}^{D}}{i_{D,\lambda 1}} \quad (2)$$

$$[A] = \frac{F_{\lambda 2}^{A}}{i_{A,\lambda 2}} \quad (3)$$

Here, ${F_{\lambda 1}}^{DA}$ is the fluorescence of the donor in the presence of the

Table 1
Parameters describing EGFR ECTM dimerization in the absence and presence of EGF. Shown are the dissociation constants, K_{diss}, and the dimerization free energies, ΔG (eq. (10), for EGFR ECTM in the absence of EGF and in the presence of 780 nM EGF. The best-fit Intrinsic FRET values, $\tilde{E}$, are also shown. The distance between the fluorescent proteins, *d,* is calculated from $\tilde{E}$ using eq. (7), under the assumption of free fluorescent protein rotation.

	K_{diss} (recs/μm²)	ΔG(kcal/mol)	$\tilde{E}$	d (nm)
ECTM EGFR	2629 ≤ 2812 ≤ 3023	−3.52 ≤ −3.48 ≤ −3.44	0.78 ≤ 0.81 ≤ 0.83	41.8 ≤ 42.8 ≤ 44.1
ECTM EGFR + EGF	15.1 ≤ 18.7 ≤ 24.6	−6.57 ≤ −6.44 ≤ −6.28	0.48 ≤ 0.49 ≤ 0.50	54.5 ≤ 54.9 ≤ 55.2

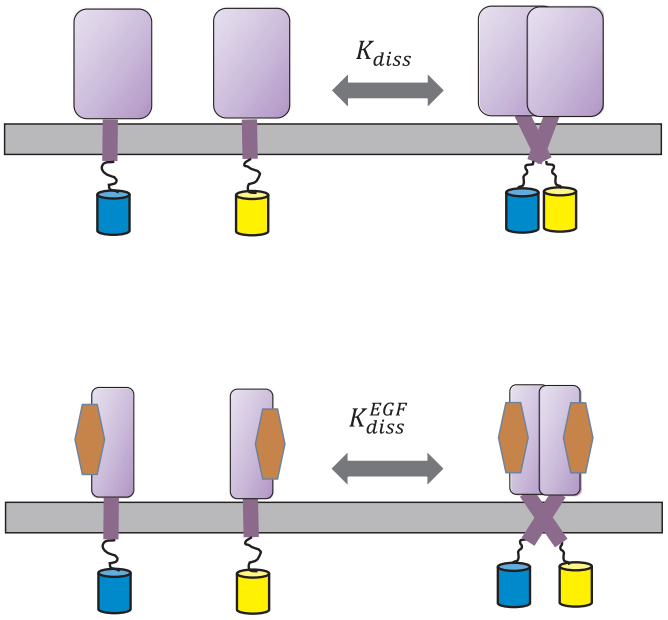

Fig. 4. Summary of results. K_{diss} is ~2800 receptors/μm^2 and K_{diss}^{EGF} is ~19 receptors/μm^2. Unliganded and ligand-bound dimers exhibit different Intrinsic FRET and thus have different TM domain dimer conformations. Not drawn to scale.

acceptor when the donor is excited at λ_1, and ${F_{\lambda 1}}^D$ is the fluorescence of the donor when it is excited at λ_1 in the absence of the acceptor. ${F_{\lambda 2}}^A$ is the fluorescence of the acceptor when excited at λ_2 in the absence of the donor. $i_{D,\,\lambda 1}$ is the slope of the calibration curve of donor fluorescence versus donor concentration at wavelength λ_1, and $i_{A,\,\lambda 2}$ is the slope of the calibration curve of acceptor fluorescence versus acceptor concentration at wavelength λ_2. ${F_{\lambda 1}}^D$ and ${F_{\lambda 2}}^A$ can be written in terms of the experimentally measured parameters as follows:

$$F_{\lambda 1}^D = F_{\lambda 1}^{DA} + \frac{Q^D}{Q^A}\left(F_{\lambda 1}^{AD} - \frac{i_{A,\lambda 1}}{i_{A,\lambda 2}}F_{\lambda 2}^A\right) \tag{4}$$

$$F_{\lambda 2}^A = \left(F_{\lambda 2}^{AD} - \frac{i_{D,\lambda 2}}{i_{D,\lambda 1}}F_{\lambda 1}^{AD}\right)\left(1 - \frac{i_{A,\lambda 1}}{i_{A,\lambda 2}}\frac{i_{D,\lambda 2}}{i_{D,\lambda 1}}\right)^{-1} \tag{5}$$

where Q_D and Q_A are the donor and acceptor quantum yields, and F^{AD} is the fluorescence of the acceptor in the presence of the donor.

4.5. FRET data analysis

The FRET efficiencies, the donor concentrations, and the acceptor concentrations were measured using the FSI-FRET software as described [28]. The FRET efficiencies were corrected for "proximity/stochastic FRET" that arises due to the random proximity of donors and acceptors in the absence of specific interactions. This correction is necessary when the fluorophores are confined to the two-dimensional plasma membrane [41–43]. The corrected FRET, E_D, is given by:

$$E_D = f_D x_A \widetilde{E} \tag{6}$$

In Eq. (6), f_D is the dimeric fraction, x_A is the acceptor fraction, and $\widetilde{E}$ is the structural parameter "Intrinsic FRET", which depends on the dimer structure, in particular, on the distance, *d,* between the fluorescent proteins in the dimer according to:

$$\widetilde{E} = \frac{1}{1 + \left(\frac{d}{R_0}\right)^6} \tag{7}$$

Here, R_o is the Förster radius of the FRET pair. For mTurq and YFP, *Ro* has been measured as 54.5 Å, assuming free fluorophore rotation [28]. The assumption of free rotation of the fluorescent proteins in our experiments is generally justified, because they are attached to the receptors via long flexible linkers. This assumption is used to calculate *d* from the best-fit Intrinsic FRET values, but it may be not entirely correct.

Following the law of mass action, the dimeric fraction can be written in terms of total receptor concentration, [T], and the dissociation constant, K_{diss}, according to Eq. 8:

$$f_D = \frac{1}{[T]}\left([T] - \frac{K_{diss}}{4}\left(\sqrt{1 + 8[T]/K_{diss}} - 1\right)\right) \tag{8}$$

Substitution of Eq. (8) in Eq. (6) yields:

$$\frac{E_D}{x_A} = \frac{1}{[T]}\left([T] - \frac{K_{diss}}{4}\left(\sqrt{1 + 8[T]/K_{diss}} - 1\right)\right)\widetilde{E} \tag{9}$$

Eq. (9) is used to fit a monomer-dimer model to the measured $\frac{E_D}{x_A}$ while optimizing for two adjustable parameters: the dissociation constant, K_{diss}, and the Intrinsic FRET, $\widetilde{E}$.

The dissociation constant, Kdiss, is reported in units of receptors/μm^2 in Table 1. The dimerization free energy ΔG (standard state defined as 1 nm^2/receptor) is calculated from the dissociation constant (when given in receptors/μm^2) as:

$$\Delta G° = RT\ \ln\left(K_{diss}/10^6\right) \tag{10}$$

Transparency document

The https://doi.org/10.1016/j.bbamem.2019.07.003 associated with this article can be found, in online version.

Declaration of Competing Interest

The authors declare no conflict of interest.

Acknowledgement

We thank Dr. D. Leahy for the EGF ligands and the EGFR ECTM plasmids. We thank M. Paul for reading the manuscript prior to publication. Supported by NSF MCB 1712740 and an NSF Graduate Research Fellowship DGE-1232825.

References

[1] W.J. Fantl, D.E. Johnson, L.T. Williams, Signaling by receptor tyrosine kinases, Annu. Rev. Biochem. 62 (1993) 453–481.
[2] M.D. Paul, K. Hristova, The RTK interactome: overview and perspective on RTK heterointeractions, Chem. Rev. 119 (2019) 5881–5921.
[3] B.C. Browne, N. O'Brien, M.J. Duffy, J. Crown, N. O'Donovan, HER-2 signaling and inhibition in breast Cancer, Curr. Cancer Drug Targets 9 (2009) 419–438.
[4] M.A. Olayioye, R.M. Neve, H.A. Lane, N.E. Hynes, The ErbB signaling network: receptor heterodimerization in development and cancer, EMBO J. 19 (2000) 3159–3167.
[5] K. Sakai, H. Yokote, K. Murakami-Murofushi, T. Tamura, N. Saijo, K. Nishio, Pertuzumab, a novel HER dimerization inhibitor, inhibits the growth of human lung cancer cells mediated by the HER3 signaling pathway, Cancer Sci. 98 (2007) 1498–1503.
[6] K. Kunii, L. Davis, J. Gorenstein, H. Hatch, M. Yashiro, A. Di Bacco, C. Elbi, B. Lutterbach, FGFR2-amplified gastric cancer cell lines require FGFR2 and Erbb3 signaling for growth and survival, Cancer Res. 68 (2008) 2340–2348.
[7] M.A. Lemmon, J. Schlessinger, Cell signaling by receptor tyrosine kinases, Cell 141 (2010) 1117–1134.
[8] L. He, K. Hristova, Physical-chemical principles underlying RTK activation, and their implications for human disease, Biochim. Biophys. Acta 1818 (2012) 995–1005.
[9] E. Li, K. Hristova, Role of receptor tyrosine kinase transmembrane domains in cell signaling and human pathologies, Biochemistry 45 (2006) 6241–6251.
[10] I. Chung, R. Akita, R. Vandlen, D. Toomre, J. Schlessinger, I. Mellman, Spatial control of EGF receptor activation by reversible dimerization on living cells, Nature 464 (2010) 783–U163.
[11] R.H. Tao, I.N. Maruyama, All EGF(ErbB) receptors have preformed homo- and heterodimeric structures in living cells, J. Cell Sci. 121 (2008) 3207–3217.

[12] C.C. Lin, F.A. Melo, R. Ghosh, K.M. Suen, L.J. Stagg, J. Kirkpatrick, S.T. Arold, Z. Ahmed, J.E. Ladbury, Inhibition of basal FGF receptor signaling by dimeric Grb2, Cell 149 (2012) 1514–1524.

[13] S. Sarabipour, K. Ballmer-Hofer, K. Hristova, VEGFR-2 conformational switch in response to ligand binding, Elife 5 (2016).

[14] M.A. Lemmon, Z.M. Bu, J.E. Ladbury, M. Zhou, D. Pinchasi, I. Lax, D.M. Engelman, J. Schlessinger, Two EGF molecules contribute additively to stabilization of the EGFR dimer, EMBO J. 16 (1997) 281–294.

[15] M. Mohammadi, S.K. Olsen, O.A. Ibrahimi, Structural basis for fibroblast growth factor receptor activation, Cytokine Growth Factor Rev. 16 (2005) 107–137.

[16] J.L. Macdonald, L.J. Pike, Heterogeneity in EGF-binding affinities arises from negative cooperativity in an aggregating system, Proc. Natl. Acad. Sci. U. S. A. 105 (2008) 112–117.

[17] D.H. Kim, S. Park, D.K. Kim, M.G. Jeong, J. Noh, Y. Kwon, K. Zhou, N.K. Lee, S.H. Ryu, Direct visualization of single-molecule membrane protein interactions in living cells, PLoS Biol. 16 (2018) e2006660.

[18] A. Wells, EGF receptor, Int. J. Biochem. Cell Biol. 31 (1999) 637–643.

[19] H.S. Wiley, S.Y. Shvartsman, D.A. Lauffenburger, Computational modeling of the EGF-receptor system: a paradigm for systems biology, Trends Cell Biol. 13 (2003) 43–50.

[20] S.H. Choi, J.M. Mendrola, M.A. Lemmon, EGF-independent activation of cell-surface EGF receptors harboring mutations found in gefitinib-sensitive lung cancer, Oncogene 26 (2007) 1567–1576.

[21] J.R. Grandis, J.C. Sok, Signaling through the epidermal growth factor receptor during the development of malignancy, Pharmacol. Ther. 102 (2004) 37–46.

[22] S. Thomson, F. Petti, I. Sujka-Kwok, D. Epstein, J.D. Haley, Kinase switching in mesenchymal-like non-small cell lung cancer lines contributes to EGFR inhibitor resistance through pathway redundancy, Clin. Exp. Metastasis 25 (2008) 843–854.

[23] S. Brunelleschi, L. Penengo, M.M. Santoro, G. Gaudino, Receptor tyrosine kinases as target for anti-cancer therapy, Curr. Pharm. Des. 8 (2002) 1959–1972.

[24] A.W. Burgess, H.S. Cho, C. Eigenbrot, K.M. Ferguson, T.P.J. Garrett, D.J. Leahy, M.A. Lemmon, M.X. Sliwkowski, C.W. Ward, S. Yokoyama, An open-and-shut case? Recent insights into the activation of EGF/ErbB receptors, Mol. Cell 12 (2003) 541–552.

[25] R. Seger, Y. Yarden, O. Kashles, D. Goldblatt, J. Schlessinger, S. Shaltiel, The epidermal growth-factor receptor as a substrate for a kinase-splitting Membranal proteinase, J. Biol. Chem. 263 (1988) 3496–3500.

[26] J.L. Macdonald-Obermann, L.J. Pike, Different epidermal growth factor (EGF) receptor ligands show distinct kinetics and biased or partial agonism for homodimer and heterodimer formation, J. Biol. Chem. 289 (2014) 26178–26188.

[27] P. Klein, D. Mattoon, M.A. Lemmon, J. Schlessinger, A structure-based model for ligand binding and dimerization of EGF receptors, Proc. Natl. Acad. Sci. U. S. A. 101 (2004) 929–934.

[28] C. King, M. Stoneman, V. Raicu, K. Hristova, Fully quantified spectral imaging reveals in vivo membrane protein interactions, Integr.Biol.(Camb.) 8 (2016) 216–229.

[29] D.R. Singh, F. Ahmed, C. King, N. Gupta, M. Salotto, E.B. Pasquale, K. Hristova, EphA2 receptor Unliganded dimers suppress EphA2 pro-tumorigenic signaling, J. Biol. Chem. 290 (2015) 27271–27279.

[30] D.R. Singh, F. Ahmed, M.D. Paul, M. Gedam, E.B. Pasquale, K. Hristova, The SAM domain inhibits EphA2 interactions in the plasma membrane, Biochim. Biophys. Acta 1864 (2016) 31–38, https://doi.org/10.1016/j.bbamcr.2016.10.011.

[31] D.R. Singh, F. Ahmed, S. Sarabipour, K. Hristova, Intracellular domain contacts contribute to Ecadherin constitutive dimerization in the plasma membrane, J. Mol. Biol. 429 (2017) 2231–2245.

[32] D.R. Singh, Q. Cao, C. King, M. Salotto, F. Ahmed, X.Y. Zhou, E.B. Pasquale, K. Hristova, Unliganded EphA3 dimerization promoted by the SAM domain, Biochem. J. 471 (2015) 101–109.

[33] D.R. Singh, P. Kanvinde, C. King, E.B. Pasquale, K. Hristova, The EphA2 receptor is activated through induction of distinct, ligand-dependent oligomeric structures, Commun. Biol. 1 (2018) 15.

[34] C. King, D. Wirth, S. Workman, K. Hristova, Cooperative interactions between VEGFR2 extracellular Ig-like subdomains ensure VEGFR2 dimerization, Biochim. Biophys. Acta 1861 (2017) 2559–2567.

[35] C. King, D. Wirth, S. Workman, K. Hristova, Interactions between NRP1 and VEGFR2 Molecules in the Plasma Membrane, (2018) (Biochim Biophys Acta Biomembr).

[36] D.M. Freed, N.J. Bessman, A. Kiyatkin, E. Salazar-Cavazos, P.O. Byrne, J.O. Moore, C.C. Valley, K.M. Ferguson, D.J. Leahy, D.S. Lidke, M.A. Lemmon, EGFR ligands differentially stabilize receptor dimers to specify signaling kinetics, Cell 171 (683–695) (2017) e618.

[37] J. Adler, A.I. Shevchuk, P. Novak, Y.E. Korchev, I. Parmryd, Plasma membrane topography and interpretation of single-particle tracks, Nat.Methods 7 (2010) 170–171.

[38] Parmryd, I., and B. Onfelt. 2013. Consequences of membrane topography. FEBS.J. 280:2775-2784.

[39] B. Sinha, D. Koster, R. Ruez, P. Gonnord, M. Bastiani, D. Abankwa, R.V. Stan, G. Butler-Browne, B. Vedie, L. Johannes, N. Morone, R.G. Parton, G. Raposo, P. Sens, C. Lamaze, P. Nassoy, Cells respond to mechanical stress by rapid disassembly of caveolae, Cell. 144 (2011) 402–413.

[40] C. King, V. Raicu, K. Hristova, Understanding the FRET signatures of interacting membrane proteins, J. Biol. Chem. 292 (2017) 5291–5310.

[41] P.K. Wolber, B.S. Hudson, An analytic solution to the Forster energy transfer problem in two dimensions, Biophys. J. 28 (1979) 197–210.

[42] B. Snyder, E. Freire, Fluorescence energy transfer in two dimensions. A numeric solution for random and nonrandom distributions, Biophys. J. 40 (1982) 137–148.

[43] C. King, S. Sarabipour, P. Byrne, D.J. Leahy, K. Hristova, The FRET signatures of non-interacting proteins in membranes: simulations and experiments, Biophys. J. 106 (2014) 1309–1317.

[44] A. Arkhipov, Y.B. Shan, R. Das, N.F. Endres, M.P. Eastwood, D.E. Wemmer, J. Kuriyan, D.E. Shaw, Architecture and membrane interactions of the EGF receptor, Cell 152 (2013) 557–569.

[45] N.F. Endres, R. Das, A.W. Smith, A. Arkhipov, E. Kovacs, Y.J. Huang, J.G. Pelton, Y.B. Shan, D.E. Shaw, D.E. Wemmer, J.T. Groves, J. Kuriyan, Conformational coupling across the plasma membrane in activation of the EGF receptor, Cell 152 (2013) 543–556.

[46] N. Del Piccolo, K. Hristova, Quantifying the interaction between EGFR dimers and Grb2 in live cells, Biophys. J. 113 (2017) 1353–1364.

[47] S. Sarabipour, K. Hristova, Mechanism of FGF receptor dimerization and activation, Nat. Commun. 7 (2016) 10262.

[48] N. Jura, N.F. Endres, K. Engel, S. Deindl, R. Das, M.H. Lamers, D.E. Wemmer, X.W. Zhang, J. Kuriyan, Mechanism for activation of the EGF receptor catalytic domain by the Juxtamembrane segment, Cell 137 (2009) 1293–1307.

[49] M.R. Brewer, S.H. Choi, D. Alvarado, K. Moravcevic, A. Pozzi, M.A. Lemmon, G. Carpenter, The Juxtamembrane region of the EGF receptor functions as an activation domain, Mol. Cell 34 (2009) 641–651.

[50] K.W. Thiel, G. Carpenter, Epidermal growth factor receptor juxtamembrane region regulates allosteric tyrosine kinase activation, Proc. Natl. Acad. Sci. U. S. A. 104 (2007) 19238–19243.

[51] F. Zhang, S. Wang, L. Yin, Y. Yang, Y. Guan, W. Wang, H. Xu, N. Tao, Quantification of epidermal growth factor receptor expression level and binding kinetics on cell surfaces by surface plasmon resonance imaging, Anal. Chem. 87 (2015) 9960–9965.

[52] S.R. Needham, S.K. Roberts, A. Arkhipov, V.P. Mysore, C.J. Tynan, L.C. Zanetti-Domingues, E.T. Kim, V. Losasso, D. Korovesis, M. Hirsch, D.J. Rolfe, D.T. Clarke, M.D. Winn, A. Lajevardipour, A.H. Clayton, L.J. Pike, M. Perani, P.J. Parker, Y. Shan, D.E. Shaw, M.L. Martin-Fernandez, EGFR oligomerization organizes kinase-active dimers into competent signalling platforms, Nat. Commun. 7 (2016) 13307.

[53] Y. Huang, S. Bharill, D. Karandur, S.M. Peterson, M. Marita, X. Shi, M.J. Kaliszewski, A.W. Smith, E.Y. Isacoff, J. Kuriyan, Molecular basis for multimerization in the activation of the epidermal growth factor receptor, Elife 5 (2016).

[54] L.R. Chen, L. Novicky, M. Merzlyakov, T. Hristov, K. Hristova, Measuring the energetics of membrane protein dimerization in mammalian membranes, J. Am. Chem. Soc. 132 (2010) 3628–3635.

[55] Low-Nam, S. T., K. A. Lidke, P. J. Cutler, R. C. Roovers, P. M. van Bergen en Henegouwen, B. S. Wilson, and D. S. Lidke. 2011. ErbB1 dimerization is promoted by domain co-confinement and stabilized by ligand binding. Nat.Struct.Mol.Biol. 18:1244–1249.

[56] V. Raicu, M.R. Stoneman, R. Fung, M. Melnichuk, D.B. Jansma, L.F. Pisterzi, S. Rath, M. Fox, J.W. Wells, D.K. Saldin, Determination of supramolecular structure and spatial distribution of protein complexes in living cells, Nat. Photonics 3 (2009) 107–113.

[57] G. Biener, M.R. Stoneman, G. Acbas, J.D. Holz, M. Orlova, L. Komarova, S. Kuchin, V. Raicu, Development and experimental testing of an optical micro-spectroscopic technique incorporating true line-scan excitation, Int. J. Mol. Sci. 15 (2014) 261–276.